

# Perturbation of a Tertiary Hydrogen Bond in Barstar by Mutagenesis of the Sole His Residue to Gln Leads to Accumulation of at Least One Equilibrium Folding Intermediate<sup>†</sup>

Utpal Nath and Jayant B. Udgaonkar\*

National Centre for Biological Sciences, TIFR Centre, P.O. Box 1234, Indian Institute of Science Campus, Bangalore 560012, India

Received August 8, 1994; Revised Manuscript Received November 7, 1994<sup>©</sup>

**ABSTRACT:** A specific tertiary hydrogen bond that is present between the side-chain hydroxyl group of Tyr30 and the side-chain N $\delta$ 1 atom of His17 in the small, monomeric, single-domain protein, barstar, has been perturbed by site-directed mutagenesis of the sole histidine residue (His17) to a glutamine residue. The effect of the perturbation has been studied in the resultant mutant protein, H17Q, by equilibrium unfolding methods. Both guanidine hydrochloride (GdnHCl)-induced denaturation and thermal denaturation studies have been performed, with unfolding monitored by UV absorption, intrinsic tryptophan fluorescence, near-UV and far-UV circular dichroism (CD), and size exclusion chromatography. While wild-type (wt) barstar shows a two-state unfolding transition when denatured by either GdnHCl or heat, the mutant protein H17Q undergoes unfolding through a transition that involves at least one equilibrium intermediate I, which is populated at intermediate concentrations of denaturant or at intermediate temperatures. In the case of GdnHCl-induced denaturation, the midpoint of the fluorescence-monitored denaturation curve is  $1.4 \pm 0.1$  M, that of the near-UV CD-monitored denaturation curve is  $1.6 \pm 0.1$  M, and that of the far-UV CD-monitored denaturation curve is  $1.8 \pm 0.1$  M. The accumulation of I is also evident in gel filtration experiments which indicate that I forms slowly from the fully-folded form, F, and that once formed, I rapidly equilibrates with the unfolded form, U. The gel filtration data for H17Q suggest that in 1.5 M GdnHCl, there is no F present and that I is the predominant form. I does not appear to possess hydrated hydrophobic surfaces, which is reflected in its inability to bind 8-anilino-1-naphthalenesulfonic acid (ANS). At least one equilibrium-unfolding intermediate is also observed upon thermal denaturation. The midpoints of the thermal denaturation curves of H17Q are  $63.0 \pm 0.5$  °C when monitored by absorbance at 287 nm or by intrinsic fluorescence at 332 nm;  $65.0 \pm 0.5$  °C when monitored by mean residue ellipticity at 275 nm; and  $68.3 \pm 0.5$  °C when monitored by mean residue ellipticity at 220 nm. In contrast, all four optical probes yield the same midpoint,  $71.5 \pm 0.5$  °C, for the wt protein. The results indicate that perturbation of the tertiary hydrogen bond leads to the accumulation of at least one intermediate (I) in both thermal denaturation studies and GdnHCl-induced denaturation studies. The intermediate(s) I are characterized by a greater disruption of tertiary structure than of secondary structure.

The mechanism by which an unfolded polypeptide chain folds to the unique, three-dimensional structure characteristic of the functional protein is poorly understood. It has now been clearly established that proteins fold along one or more well-defined pathways, which involve intermediate structures that are only partly-folded (Kim & Baldwin, 1990; Matthews, C. R., 1993). Such kinetic intermediates are difficult to study because of the transience of their presence on the kinetic folding pathway, in spite of the development of new methodologies (Udgaonkar & Baldwin, 1988; Roder *et al.*, 1988; Matouschek & Fersht, 1991; Evans & Radford, 1994). Nevertheless, the study of partly-folded intermediate structures is essential to understand the complex protein-folding reaction, and it is therefore important to be able to study partly-folded structures under equilibrium conditions.

Folding intermediates are usually populated to a negligible extent at equilibrium because they are less stable than the fully-folded protein. Thus, many of the small monomeric, single-domain proteins that are traditionally used as model proteins for folding studies unfold through a highly cooperative process that can be analyzed according to a two-state  $U \rightleftharpoons F$  model not involving any intermediate between the fully-folded (F)<sup>1</sup> and unfolded (U) forms of the protein (Privalov, 1992). A few proteins do, however, undergo unfolding through an equilibrium intermediate state, I (Ptitsyn, 1992), and therefore follow a three-state  $U \rightleftharpoons I \rightleftharpoons F$  model for folding. Partly-folded structures are more commonly observed at extremes of pH, temperature, or ionic strength where they usually manifest themselves as molten globules

<sup>†</sup> This work was funded by the Tata Institute of Fundamental Research and in part by the Department of Biotechnology, Government of India.

\* Corresponding author; Fax: 91-080-3343851; e-mail address: jayant@tifrbng.ernet.in or jayant@tifrvax.bitnet.

<sup>©</sup> Abstract published in *Advance ACS Abstracts*, January 1, 1995.

<sup>1</sup> Abbreviations: F, fully-folded form; U, unfolded form; I, collection of one or more intermediate forms of barstar; GdnHCl, guanidine hydrochloride; DTT, dithiothreitol; ANS, 8-anilino-1-naphthalenesulfonic acid; CD, circular dichroism; NMR, nuclear magnetic resonance; PCR, polymerase chain reaction; UV, ultraviolet; H17Q, a His17→Gln17 mutant form of barstar; BSCCAA, a Cys40Cys82→Ala40Ala82 double mutant form of barstar.

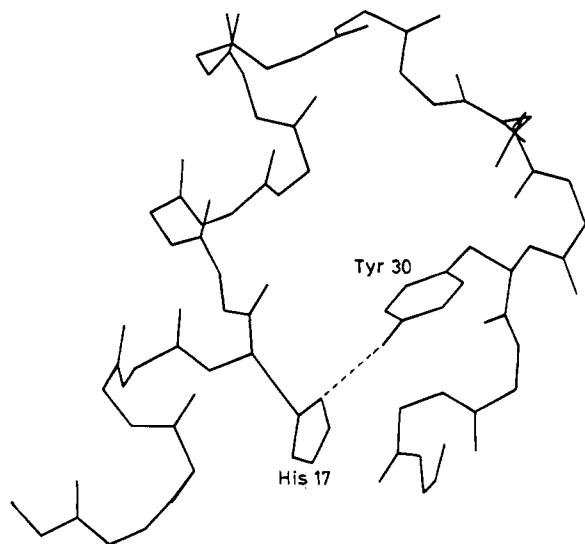


FIGURE 1: Conformation of His17 and Tyr30 in barstar (Guillet *et al.*, 1993). The polypeptide segment comprising amino acid residues 12–33 and encompassing helix 1 and the loop connecting helix 1 to helix 2 is shown. For clarity, the side chains of only His17 and Tyr30 are shown. The distance between the side chain hydroxyl oxygen atom of Tyr30 and the N $\delta$ 1 atom of the side chain of His17 is 2.7 Å.

(Kuwajima, 1992; Ptitsyn, 1992; Dobson, 1994), retaining considerable native-like secondary structure but little tertiary structure. Again, because of the difficulty in studying kinetic intermediates, there is only little direct evidence that molten globule-like intermediates form on the folding pathway leading to the functional, native structure of the protein.

Site-directed mutagenesis is a potential method for breaking down the cooperativity of the folding process so that folding intermediates are populated at equilibrium and are more amenable to study (Zitzewitz & Matthews, 1993). Perturbing a strong tertiary interaction between two units of secondary structure that can fold independently is expected to alter the cooperativity of the folding process. In this work, such an approach has been used to populate at least one equilibrium folding intermediate in the GdnHCl-induced and thermally-induced unfolding of the small 89 residue protein barstar, which is a single-domain protein formed from four  $\alpha$ -helices and a three-stranded parallel  $\beta$ -sheet (Guillet *et al.*, 1993) and which is an attractive model protein for folding studies.

A specific tertiary interaction is present between Tyr30, a residue on the loop between helix 1 (residues 12–25) and helix 2 (residues 33–44), and His17, the sixth residue on helix 1 (Guillet *et al.*, 1993; Mauguen, Y., personal communication): the Tyr30 OH is hydrogen-bonded to His17 N $\delta$ 1 (Figure 1). This interaction has been perturbed by site-directed mutagenesis of His17 to Gln. It is shown here that in this mutant protein, H17Q, the stability of the tertiary structure is reduced to a greater extent than that of the secondary structure. The GdnHCl-induced folding transition as well as the thermally-induced folding transition is altered from a two-state U  $\rightleftharpoons$  F transition in the wt protein (Khurana & Udgaonkar, 1994; Shastry *et al.*, 1994) to a U  $\rightleftharpoons$  I  $\rightleftharpoons$  F transition in H17Q, where I represents one or more folding intermediates. The existence of I is seen in the non-coincidence of unfolding transitions monitored by three different optical probes of structure and also in gel filtration

experiments. I appears to have considerable secondary structure but has a disrupted tertiary structure.

## MATERIALS AND METHODS

**Chemicals.** GdnHCl, GpG, ANS, yeast *Torula* RNA, and chromatographic resins were obtained from Sigma; SP-Trisacryl was from IBF; and dialysis tubes of  $M_r$  3500 cutoff were from Spectrum Medical Industries. *Taq* polymerase was from Boehringer Mannheim, and restriction enzymes were from New England Biolab. DNA sequencing was done using Sequenase Version 2.0 obtained from United States Biochemicals. All other chemicals were of analytical grade.

**Bacterial Strains, Plasmids, and Site-Directed Mutagenesis.** The *Escherichia coli* strain used for protein expression was MM294 (*supE44 hsdR endA1 pro thi*). The barnase and barstar expression plasmids, pMT416 and pMT316, respectively, were kindly provided by Hartley (1988). Oligonucleotide-directed mutagenesis was done by PCR, as described by Merino *et al.* (1992). The mutagenic primer used to replace His17 to Gln was AGC GAC CTC CAA\* CAG ACA T (asterisk follows the mismatch). The three end-primers were ACA CAG GAA ACA GGA TCC GT, AAG GCC TTG TCG ACC CCC ATT ACG CCA AGC TTG GGG, and AAG GCC TTG TCG ACC CCC. Primers were synthesized on an Applied Biosystems 391 DNA synthesizer. The mutagenesis was done on plasmid pMT316, the barstar expression plasmid. After the first round of PCR, the product was separated in a 2% agarose gel and eluted out by electroelution. After the second round of PCR, the mutated product was cloned back into the pMT316 lacking the wt gene between the *Bam*HI and *Hind*III sites. Transformation was carried out by the usual procedure (Sambrook *et al.*, 1989). The mutation was verified by dideoxy sequencing (Sanger *et al.*, 1977) of the entire mutant barstar gene.

**Expression and Purification of Barstar and Barnase.** The procedure for the purification of H17Q was similar to that described earlier for wt barstar (Khurana & Udgaonkar, 1994), except that an additional gel filtration step using a Sephadex G-50 column was necessary because the yield of H17Q, at 2 mg/L *E. coli* growth, was less than 1% of that of wt barstar. Barnase was purified as described by Paddon and Hartley (1987) and Mossakowska *et al.* (1989); the yield obtained was 8 mg/L.

The purity of each protein preparation was checked by SDS-PAGE (Schagger & von Jagow, 1987). Barstar was found to be >98% pure whereas the purity of barnase was >95%. Protein concentration was determined by a colorimetric assay (Bradford, 1976), and the extinction coefficient of H17Q was determined to have the same value as that of wt barstar, namely, 23 000 M $^{-1}$  cm $^{-1}$  (Khurana & Udgaonkar, 1994).

**Inhibition Assay for Barstar Using GpG as Substrate.** This was done following the procedure of Mossakowska *et al.* (1989). The concentration of GpG used in the assays was 100  $\mu$ M and was estimated from its change in extinction coefficient at 280 nm on degradation by barnase ( $\Delta\epsilon_{280} = 1500$  M $^{-1}$  cm $^{-1}$ ) (Osterman & Waltz, 1978). The substrate dissolved in buffer (50 mM MOPS, 1 mM DTT, 1 mM EDTA, pH 7.0) was put into the cuvette and equilibrated at 25 °C for 2 min. Appropriately diluted barnase and barstar were mixed outside, incubated at 25 °C for 2 min, and added

to the cuvette. The hydrolysis of GpG was monitored at 280 nm in a Cary 1 spectrophotometer.

**Buffers and Solutions.** All buffers were of the highest purity grade. Buffers used for equilibrium studies, including gel filtration studies, contained 20 mM sodium phosphate, 0.2 M KCl, 0.5 mM EDTA, and 0.5 mM DTT at pH 7. For far-UV CD work, 200  $\mu$ M DTT was used instead of 500  $\mu$ M. The same buffer was used for temperature melts but without KCl. For pH titrations, a buffer consisting of 2 mM sodium citrate, 2 mM sodium phosphate, 2 mM sodium borate, 1 mM EDTA, and 1 mM DTT was used over the pH range 2–9. All buffers were passed through 0.22- $\mu$ m filters and degassed before use. ANS binding studies were carried out as described by Khurana and Udgaonkar (1994). The concentration of the GdnHCl stock solution was checked by measurement of the refractive index (Pace *et al.*, 1989). All experiments were done in reducing conditions, *i.e.*, in the presence of at least 20-fold excess DTT, which prevents the small amount of (<3%) dimer formation through an intermolecular disulfide bond that is seen in nonreducing conditions (Shastry *et al.*, 1994). The two cysteine residues in barstar have a low solvent accessibility and are too far apart to form an intramolecular disulfide bond (Guillet *et al.*, 1993; Lubinski *et al.*, 1994).

**Equilibrium Unfolding Studies.** Equilibrium unfolding as a function of GdnHCl concentration was monitored by far-UV CD, near-UV CD, and fluorescence. In each case, the protein was equilibrated for at least 15 h prior to the measurement. CD studies were done on a Jasco J720 spectropolarimeter. Spectra were collected with a band width of 1 nm, response time of 1 s, and scan speed of 20 nm/min. Each spectrum was the average of at least 10 scans. For denaturation studies, secondary structure was monitored at 220 nm and tertiary structure was monitored at 275 nm. Measurements were made with protein concentrations of 20 (far-UV) and 50  $\mu$ M (near-UV) with cuvettes of path length 0.1 (far-UV) and 1 cm (near-UV).

Fluorescence studies were done using a Shimadzu spectrofluorimeter. For studying the intrinsic fluorescence, the protein was excited at 287 nm, and emission was monitored at 332 nm with a band width of 5 nm for excitation and emission. All experiments were done at 25 °C. Measurements were made with a protein concentration of 4  $\mu$ M or less and a 1.0 cm path length cuvette.

**Size Exclusion Chromatography.** The hydrodynamic properties of H17Q and wt barstar as a function of GdnHCl concentration were studied using gel filtration on both a Superdex 75 HR 10/30 column and a Superose 6 HR 10/30 column using a Pharmacia FPLC system. The protein was equilibrated in buffer (20 mM sodium phosphate, 0.2 M KCl, 1 mM EDTA, 1 mM DTT, pH 7, and varying concentrations of GdnHCl) for 15 h prior to the chromatography run. The column was equilibrated with the same buffer by passing four column volumes of the buffer through it prior to injecting 100  $\mu$ L of 20  $\mu$ M protein solution. In some experiments, the time of prior equilibration was varied from 0 to 15 h. The flow rates used were 0.5 (Superdex) and 0.3 mL/min (Superose).

**Thermal Denaturation.** Thermal denaturation of H17Q or wt barstar was done in 20 mM phosphate, 100  $\mu$ M DTT, and 250  $\mu$ M EDTA, pH 7.0. Denaturation was followed by monitoring absorbance at 287 nm in a Cary 1 spectrophotometer equipped with a Cary peltier heating/cooling acces-

sory device and a Cary thermistor temperature probe accessory, or by monitoring mean residue ellipticities at 220 (far-UV) and 275 nm (near-UV) in a Jasco J720 spectropolarimeter interfaced with a Neslab RTE-110 circulating bath. The heating rate used was 0.33 °C/min. Using a heating rate of 0.16 °C/min yielded identical denaturation curves. In all cases, the temperature of the protein solution was monitored with a probe placed directly in the cuvette.

**Data Analysis.** Raw equilibrium denaturation data were converted to plots of  $f_{app}$  versus denaturant concentration using

$$f_{app} = \frac{Y_O - (Y_F + m_F[D])}{(Y_U + m_U[D]) - (Y_F + m_F[D])} \quad (1)$$

$Y_O$  is the observed signal at a particular GdnHCl concentration.  $Y_F$  and  $Y_U$  represent the intercepts, and  $m_F$  and  $m_U$  are the slopes of the native and the unfolded baselines, respectively, and were obtained by extrapolation of linear least-squares fits of the baselines.

To determine whether the application of a two-state  $F \rightleftharpoons U$  unfolding model was appropriate for analyzing the GdnHCl-induced denaturation data,  $f_{app}$  values were fit to

$$f_{app} = \frac{\exp\left[\frac{-(\Delta G + m_G[D])}{RT}\right]}{1 + \exp\left[\frac{-(\Delta G + m_G[D])}{RT}\right]} \quad (2)$$

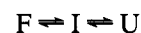
In eq 2,  $f_{app}$  is related to  $\Delta G$  by a transformation of the Gibbs–Helmholtz equation in which the equilibrium constant for unfolding in the folding transition zone,  $K_{app}$ , is given by  $K_{app} = f_{app}/(1 - f_{app})$ , for a two-state transition.

Raw equilibrium denaturation data were also directly fitted to a two-state  $F \rightleftharpoons U$  unfolding model, using eq 3 (Santoro & Bolen, 1988). In eq 3, the baselines are fit simultaneously with the unfolding transition.

$$Y_O = \frac{Y_F + m_F[D] + (Y_U + m_U[D])\exp\left[\frac{-(\Delta G + m_G[D])}{RT}\right]}{1 + \exp\left[\frac{-(\Delta G + m_G[D])}{RT}\right]} \quad (3)$$

A three-state model for unfolding was used for a more proper analysis of GdnHCl-induced denaturation curves for H17Q:

mechanism 1



where F and U are the fully-folded and unfolded forms of the protein, and I is an intermediate that is populated at equilibrium. The  $I \rightleftharpoons F$  and  $U \rightleftharpoons I$  equilibria are characterized by the equilibrium constants  $K_{IF}$  ( $=I/F$ ) and  $K_{UI}$  ( $=U/I$ ), and the free energy changes  $\Delta G_{IF}$  and  $\Delta G_{UI}$ , respectively.

For the three-state model,  $f_{app}$  is given by the following equation (Garvey & Matthews, 1989):

$$f_{\text{app}} = \frac{Z_1 \exp\left[\frac{-\Delta G_{\text{IF}}}{RT}\right] + \exp\left[\frac{-(\Delta G_{\text{IF}} + \Delta G_{\text{UI}})}{RT}\right]}{1 + \exp\left[\frac{-\Delta G_{\text{IF}}}{RT}\right] + \exp\left[\frac{-(\Delta G_{\text{IF}} + \Delta G_{\text{UI}})}{RT}\right]} \quad (4)$$

where  $Z_1$  is a parameter that measures the optical characteristics of the intermediate I in relation to that of F and U and is given by

$$Z_1 = \frac{Y_I - Y_F}{Y_U - Y_F} \quad (5)$$

For denaturation by GdnHCl, it has been assumed that the free energies of unfolding of F and I both show a linear dependence on the denaturant concentration (Schellman, 1978):

$$\Delta G_{\text{UF}} = \Delta G_{\text{UF}}(H_2O) + m_G[D] \quad (6)$$

$$\Delta G_{\text{IF}} = \Delta G_{\text{IF}}(H_2O) + m_{\text{IF}}[D] \quad (7)$$

$$\Delta G_{\text{UI}} = \Delta G_{\text{UI}}(H_2O) + m_{\text{UI}}[D] \quad (8)$$

pH titrations were modeled on the protonation/deprotonation of a single titratable group (Khurana & Udgaonkar, 1994):

$$Y(\text{pH}) = \frac{Y_d + Y_p 10^{\text{pH}-\text{pH}_m}}{1 + 10^{\text{pH}-\text{pH}_m}} \quad (9)$$

where  $Y(\text{pH})$  is the spectroscopic property being measured at a particular pH value,  $Y_d$  and  $Y_p$  are the spectroscopic properties characteristic of the deprotonated and protonated states respectively, and  $\text{pH}_m$  is the midpoint of the observed titration.

To obtain the value of the observed midpoint from a thermal denaturation curve, the first derivative of the optical signal with respect to temperature was first determined, and the observed midpoint was determined as the value at which the first derivative exhibited a maximum value (CD-monitored denaturation curves) or a minimum value (fluorescence- and absorbance-monitored denaturation curves).

## RESULTS

**Structure and Activity of H17Q.** Figure 2 compares the structure and activity of the mutant protein H17Q to those of wt barstar. The far-UV spectrum of H17Q is virtually identical to that of the wt protein (Figure 2a), and the mean residue ellipticity at 220 nm, which is a measure of the helicity of the protein, is only marginally greater for H17Q. The near-UV spectra (Figure 2b), which measure the asymmetric environments of aromatic groups, are also similar, although the magnitude of the signal is 30% greater for the mutant. The difference in the environments of the aromatic groups in H17Q and in the wt protein is also reflected in the UV absorption difference spectra (Figure 2c). H17Q undergoes a larger change in absorption at 287 nm on unfolding in 6 M GdnHCl than does the wt protein. The intrinsic tryptophan fluorescence intensity of H17Q at the wavelength of maximum emission, 332 nm, is 90% of that of the wt barstar (data not shown). Figure 2d indicates that

the activity of H17Q is approximately 80% of the activity of wt barstar.

**GdnHCl-Induced Denaturation Curves.** In Figure 3 are shown GdnHCl-induced denaturation curves monitored by three different probes; fluorescence, near-UV CD, and far-UV CD. The first two are probes of tertiary structure, while the latter measures secondary structure. When monitored by fluorescence, tertiary structure is half-unfolded at a GdnHCl concentration of  $1.4 \pm 0.1$  M, and when monitored by near-UV CD, tertiary structure is half-unfolded at a GdnHCl concentration of  $1.6 \pm 0.1$  M. Secondary structure is half-unfolded at a GdnHCl concentration of  $1.8 \pm 0.1$  M. The unfolding transitions of H17Q, like those of wt barstar (Khurana & Udgaonkar, 1994), are found to be completely reversible (data not shown).

The observation that the midpoints of the unfolding transitions of H17Q were different when determined using different optical probes suggested that the unfolding of H17Q did not follow a two-state  $F \rightleftharpoons U$  model. To confirm this, each of the three differently monitored unfolding transitions shown in Figure 3 was analyzed according to such a model using eqs 2 and 3. The values obtained from these two-state analyses for  $C_m$  and  $m_G$ , the midpoint and the slope, respectively, of the unfolding transition were 1.4 M and  $-1.6$  kcal mol<sup>-1</sup> M<sup>-1</sup> (fluorescence), 1.65 M and  $-2.2$  kcal mol<sup>-1</sup> M<sup>-1</sup> (near-UV CD), and 1.8 M and  $-1.1$  kcal mol<sup>-1</sup> M<sup>-1</sup> (far-UV CD). The significant disagreement between the midpoints and slopes of the transitions, when monitored by different optical probes, constitutes strong evidence for intermediates in unfolding. Thus, a two-state analysis of the GdnHCl-induced denaturation curves of H17Q is not appropriate, and a three-state analysis according to a  $F \rightleftharpoons I \rightleftharpoons U$  model for unfolding was attempted.

An analysis of the three denaturation curves using the three-state model (eq 4) was attempted in three different ways. First, with the assumptions that the fluorescence of I is the same as that of U and that the secondary structure of I is the same as that of F, eq 4 was used with  $Z_1$  set to 1 for analyzing the fluorescence-monitored denaturation curve; the equation then describes the loss of tertiary structure. Similarly, eq 4 was used with  $Z_1$  set to 0 for analyzing the far-UV CD-monitored denaturation curve; the equation then describes the loss of secondary structure. Then, because of the large number of variables, a simulated fitting of the fluorescence and far-UV CD data to eqs 4 and 5 and 7 and 8 was carried out. Although the simulated fits to the fluorescence and far-UV CD data were good (see Figure 3), the values for  $\Delta G_{\text{IF}}$ ,  $\Delta G_{\text{UI}}$ ,  $m_{\text{IF}}$ , and  $m_{\text{UI}}$  obtained could not be used to carry out a simulated fit to the near-UV CD data, even when the value for  $Z_1$  was varied between 0 and 1. In another attempt to fit the data in Figure 3 to eq 4, it was attempted to carry out a simulated global fit to all three denaturation curves by simultaneously varying all five parameters in eq 4. This attempt was also not successful. In a third attempt, the values of  $f_{\text{app}}$  at 1.5 M GdnHCl for the three curves in Figure 3 were taken as the respective values for  $Z_1$  (see Discussion), but this attempt was also not successful. Thus, it appears that a three-state  $U \rightleftharpoons I \rightleftharpoons F$  transition in which I represents a single unique intermediate cannot account for the data in Figure 3, and I probably represents a collection of folding intermediates.

**Size Exclusion Chromatography.** In Figure 4a is shown the elution volumes of wt barstar and H17Q on a Superdex

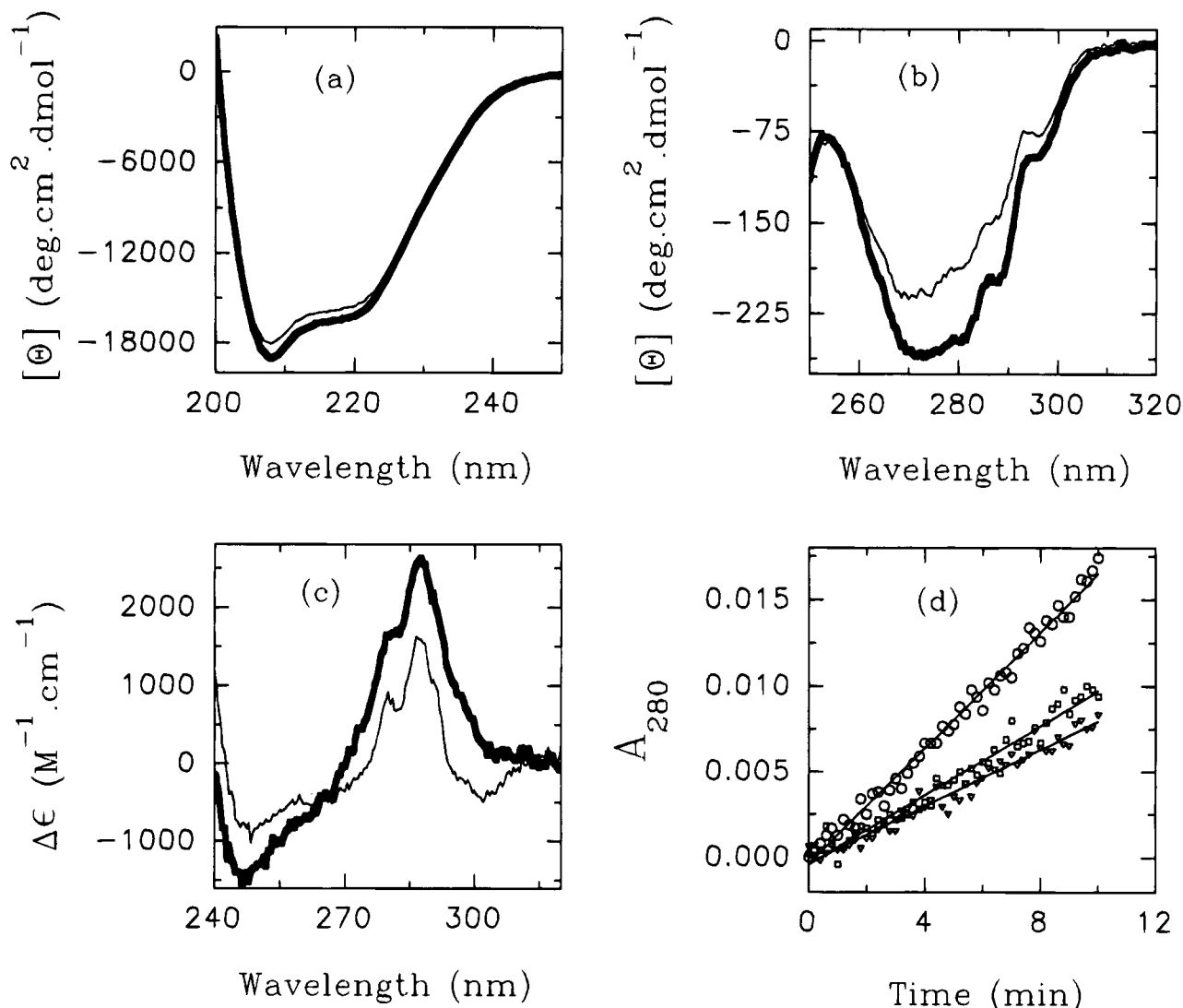


FIGURE 2: (a) Far-UV spectra of H17Q and wt barstar at pH 7, 25 °C. The value of  $\theta_{220}$  is  $-15500^{\circ} \text{ cm}^2 \text{ dmol}^{-1}$  for wt barstar and  $-16000^{\circ} \text{ cm}^2 \text{ dmol}^{-1}$  for H17Q. (b) Near-UV spectra of H17Q and wt barstar at pH 7, 25 °C. The value of  $\theta_{275}$  is  $-200^{\circ} \text{ cm}^2 \text{ dmol}^{-1}$  for wt barstar and  $-260^{\circ} \text{ cm}^2 \text{ dmol}^{-1}$  for H17Q. (c) UV difference absorption spectra of H17Q and wt barstar at pH 7, 25 °C.  $\Delta\epsilon_{287}$  for unfolding in 6 M GdnHCl is equal to  $1600 \text{ M}^{-1} \text{ cm}^{-1}$  for wt barstar and  $2600 \text{ M}^{-1} \text{ cm}^{-1}$  for H17Q. The thick lines in panels a–c represent data for H17Q, while the thin lines represent data for wt barstar. (d) Activity assays for wt barstar and H17Q at 25 °C. The inhibition by barstar of the barnase-catalyzed degradation of GpG was measured by monitoring the increase in absorbance at 280 nm which accompanies the reaction. (○) Activity of 1  $\mu\text{M}$  barnase. (▽) Activity of 1  $\mu\text{M}$  barnase + 0.25  $\mu\text{M}$  wt barstar. (◻) Activity of 1  $\mu\text{M}$  barnase + 0.25  $\mu\text{M}$  H17Q.

75 gel filtration column as a function of GdnHCl concentration. For both proteins, a single elution peak was observed, which moved to smaller elution volumes as the concentration of GdnHCl was increased. The dependence of the elution volume on the concentration of GdnHCl for H17Q is markedly different from that for wt barstar. In the presence of low concentrations of GdnHCl, both wt barstar and H17Q eluted out at elution volumes larger than in 0 M GdnHCl. This artifact in the case of the Superdex 75 column has also been previously reported for barnase in the presence of low concentrations of urea (Sanz & Fersht, 1993) and has been attributed to nonspecific hydrophobic interactions with the gel matrix. The experiment was therefore repeated with a Superose 6 column, but the same artifact was observed (Figure 4b). Neither protein exhibits a CD-detectable conformational change in the range of GdnHCl concentration affected by the artifact. With either column, the elution volumes of wt barstar and H17Q do not significantly differ in the absence of GdnHCl or in the presence of GdnHCl at

concentrations greater than 3 M. Above 3 M GdnHCl, where both proteins are completely denatured (Figure 3), the decrease in elution volume is probably due to swelling of the denatured state (Uversky & Ptitsyn, 1994). The presence of only a single elution peak at any concentration of GdnHCl indicates that equilibration between the fully-folded and unfolded forms (and any equilibrium intermediates, if present) is very fast compared to the time of chromatography. The elution volumes observed in Figure 4a,b therefore represent the weighted average of all forms present at equilibrium. The elution peaks for H17Q and wt barstar in 0 and 6 M GdnHCl were narrow, but were broader in the middle of the folding transition zone. This broadening was significantly more in the case of H17Q than in the case of wt barstar.

Figure 5a shows the dependence of the elution profile of H17Q in 1.5 M GdnHCl on the time of prior incubation in the same buffer. A Superdex 75 column was used because it provided better resolution. The protein was incubated for

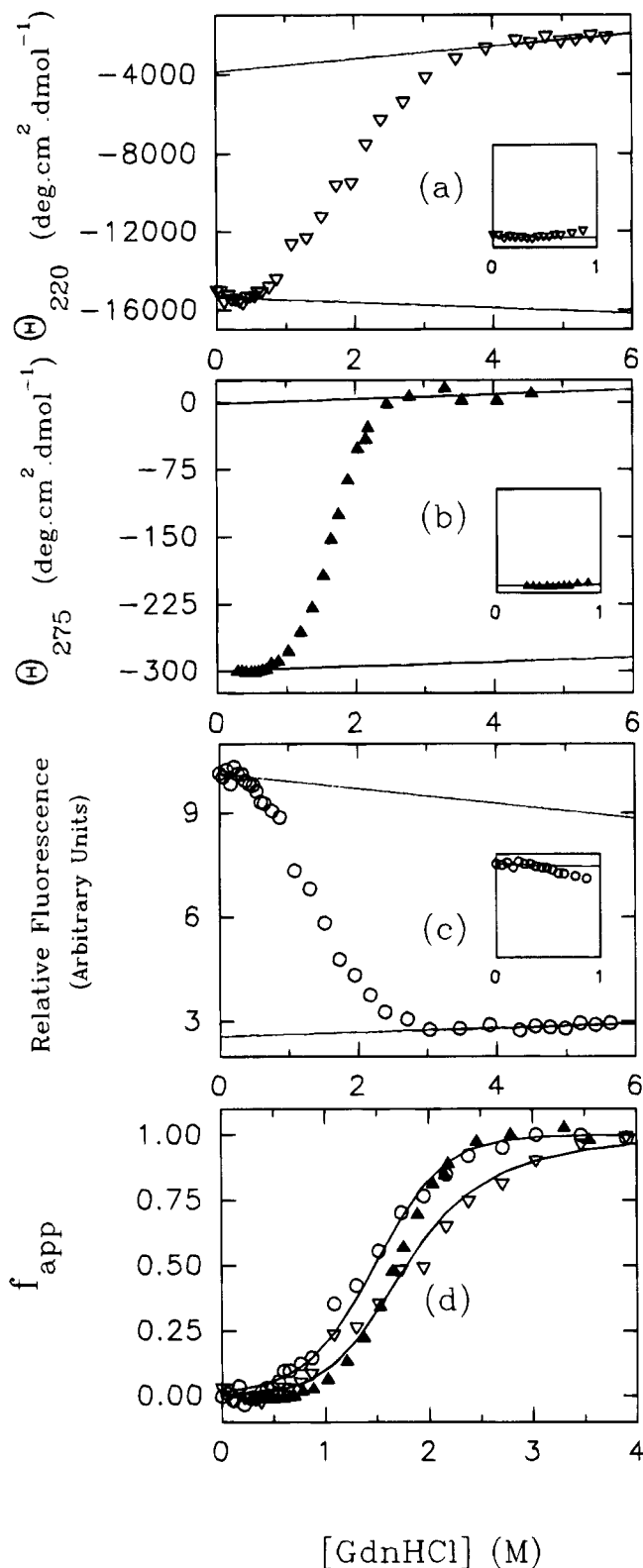


FIGURE 3: Equilibrium denaturation curves of H17Q at 25 °C, pH 7. (a) GdnHCl-induced denaturation was followed by monitoring mean residue ellipticity at 220 nm. (b) GdnHCl-induced denaturation was followed by monitoring mean residue ellipticity at 275 nm. (c) GdnHCl-induced denaturation was followed by monitoring relative fluorescence at 332 nm on excitation at 287 nm. The solid lines in panels a–c are least-squares fits of the folding and unfolding zone baselines. The insets in panels a–c show the folding baseline regions in the GdnHCl concentration range 0–1 M. The vertical ranges in the insets are the same as in the main figures. (d) The data in panels a–c were converted to  $f_{app}$  values using eq 1 and are plotted against GdnHCl concentration. The solid lines through the far-UV CD data (∇) and the fluorescence data (○) are nonlinear least-squares fits of data to eq 4, with  $Z_I$  set to 1 for the fluorescence data and to 0 for the far-UV CD data, and yielded values for  $\Delta G_{UI}$ ,  $\Delta G_{IF}$ ,  $m_{UI}$ , and  $m_{IF}$  of 2.5 kcal mol<sup>-1</sup>, 0.7 kcal mol<sup>-1</sup>, -1.3 kcal mol<sup>-1</sup> M<sup>-1</sup>, and -0.7 kcal mol<sup>-1</sup> M<sup>-1</sup>, respectively. The near-UV CD data (▲) could not be fit by simulation to eq 4 using these values for  $\Delta G_{UI}$ ,  $\Delta G_{IF}$ ,  $m_{UI}$ , and  $m_{IF}$  and any value for  $Z_I$ .

varying periods of time in 1.5 M GdnHCl, and a 100- $\mu$ L aliquot was loaded onto the column at each of the times

indicated. Two elution peaks, one at 14.8 mL and the other at 14 mL, are seen. The peak at 14 mL increases in area at

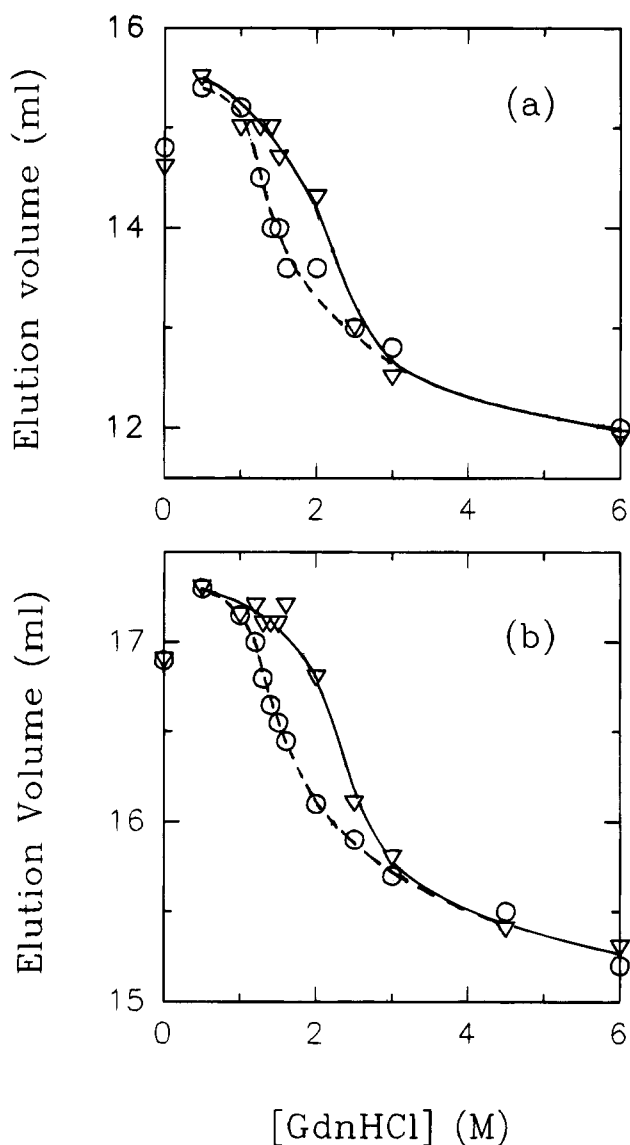


FIGURE 4: Dependences of the elution profiles of wt barstar and H17Q at 25 °C on GdnHCl concentration. A Superdex 75 column was used in panel a and a Superose 6 column was used in panel b. (○) H17Q; (▽) wt barstar. Protein solutions were incubated in the indicated concentrations of GdnHCl for 20 h before gel filtration in the column equilibrated with the same concentration of GdnHCl. Equal concentrations of both proteins (20  $\mu$ M) were used in all chromatography runs.

the expense of the other peak with the time incubation in 1.5 M GdnHCl, and at 900 min only the former is seen. The presence of two peaks in slow equilibration with each other at the shorter times of incubation indicate that there are at least two forms of the protein in very slow equilibrium with each other. The elution peak at 14 mL does not correspond to the peak of fully-unfolded protein (see Figure 4a), and it therefore represents a form of H17Q more compact than U but less compact than F. The peak at 14 mL cannot be an aggregated form of H17Q, because when fully-folded barstar is allowed to dimerize through an intermolecular disulfide bond in the absence of DTT (see Materials and Methods), this dimer elutes out at 13.4 mL, and a similarly formed dimer in 6 M GdnHCl elutes out at 10.1 mL (S. Ramachandran and J. B. Udgaonkar, unpublished results).

In Figure 5b, the relative areas of the two peaks are plotted as a function of time of incubation in 1.5 M GdnHCl. The relative area of the 14.8-mL peak decreases in two kinetic

phases. One phase is over within 3 min, the earliest time of chromatography. The slower phase occurs with an apparent rate of  $6.7 \times 10^{-5} \text{ s}^{-1}$ , and the relative area of the 14-mL peak increases at the same apparent rate. In the case of wt barstar, a single peak is seen at all times of incubation (data not shown).

**ANS Binding Studies.** ANS binds to hydrated hydrophobic surfaces in proteins (Stryer, 1965), which are commonly seen in molten globule conformations (Ptitsyn, 1992). Such binding leads to a large increase in the fluorescence of ANS as well as a blue shift in its emission maximum from 530 to 470 nm. The addition of 10  $\mu$ M ANS to 1  $\mu$ M H17Q in either 0, 1.5, 2, 3, or 6 M GdnHCl at pH 7 does not lead to an increase in fluorescence at 470 nm: there is no difference in the fluorescence between H17Q, wt barstar, or a sample without any protein (data not shown). This result indicates that I does not possess a common property shared by many but not all molten globules, that of possessing accessible hydrated hydrophobic surfaces to which ANS can bind. The increase in fluorescence is, however, seen at pH 3 where both wt barstar (Khurana & Udgaonkar, 1994) and H17Q (unpublished results) exist in molten globule-like conformations.

**Thermal Denaturation.** Figure 6 shows thermal melts for both wt barstar and H17Q, using near-UV and far-UV CD as probes to monitor unfolding. It is seen that for wt barstar the same value for the midpoint of the thermal transition,  $T_m$ , is obtained ( $71.5 \pm 0.5 \text{ }^\circ\text{C}$ ) with both these structural probes. The midpoint of the transition is also the same when absorption at 287 nm is used to monitor the unfolding transition (data not shown). The  $T_m$  is lower for H17Q when measured by either probe: it is  $65 \pm 0.5 \text{ }^\circ\text{C}$  when monitored by near-UV CD and  $68 \pm 0.5 \text{ }^\circ\text{C}$  when monitored by far-UV CD. Fluorescence-monitored ( $\lambda_{\text{exc}} = 287 \text{ nm}$ ;  $\lambda_{\text{emm}} = 332 \text{ nm}$ ) and absorbance-monitored ( $\lambda_{\text{abs}} = 287 \text{ nm}$ ) thermal melts for H17Q yielded the same values for  $T_m$  of  $63 \pm 0.5 \text{ }^\circ\text{C}$ . The protein concentration used in the latter (100  $\mu$ M) was more than 20-fold higher than that used in the former (5  $\mu$ M). Thus, it is unlikely that thermal denaturation of H17Q is affected by the concentration of protein used.

**pH Titrations.** Figure 7 shows the dependence of the fluorescence of H17Q on pH. The increase in fluorescence that is observed could be satisfactorily fit to eq 9. Thus, only one titratable group is observed to deprotonate with an increase in pH from 2 to 9. The apparent  $\text{pK}_a$  of this titratable group was determined to be  $5.0 \pm 0.2$  in both H17Q (Figure 7) and wt barstar (data not shown). The titration of this group was also monitored using mean residue ellipticity at 220 nm (data not shown), and the same value was obtained for the apparent  $\text{pK}_a$ .

## DISCUSSION

Folding intermediates can be populated at equilibrium if the fully-folded protein is sufficiently destabilized with respect to the intermediate. Such destabilization can be achieved in several ways. For proteins that need a bound cofactor or metal ion to function, removal of the cofactor or metal ion often sufficiently destabilizes the fully-folded protein so that folding intermediates are populated at equilibrium. For example, removal of the heme group in myoglobin (Kirby & Steiner, 1970; Barrick & Baldwin, 1993) or calcium ions in  $\alpha$ -lactalbumin (Kuwajima *et al.*,

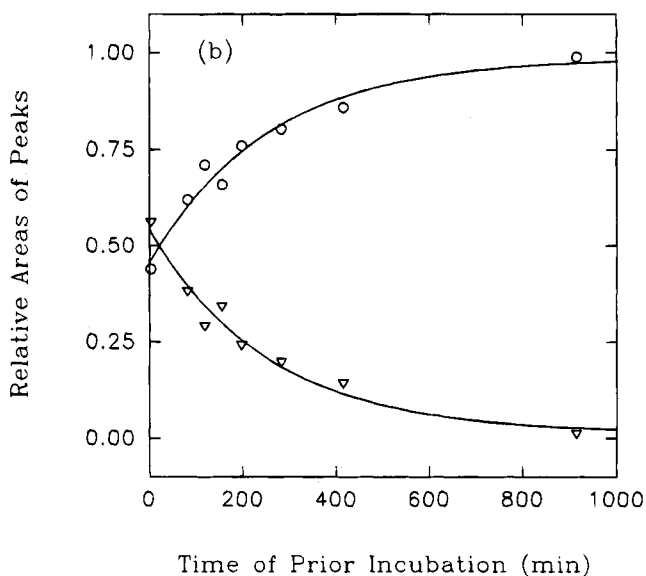
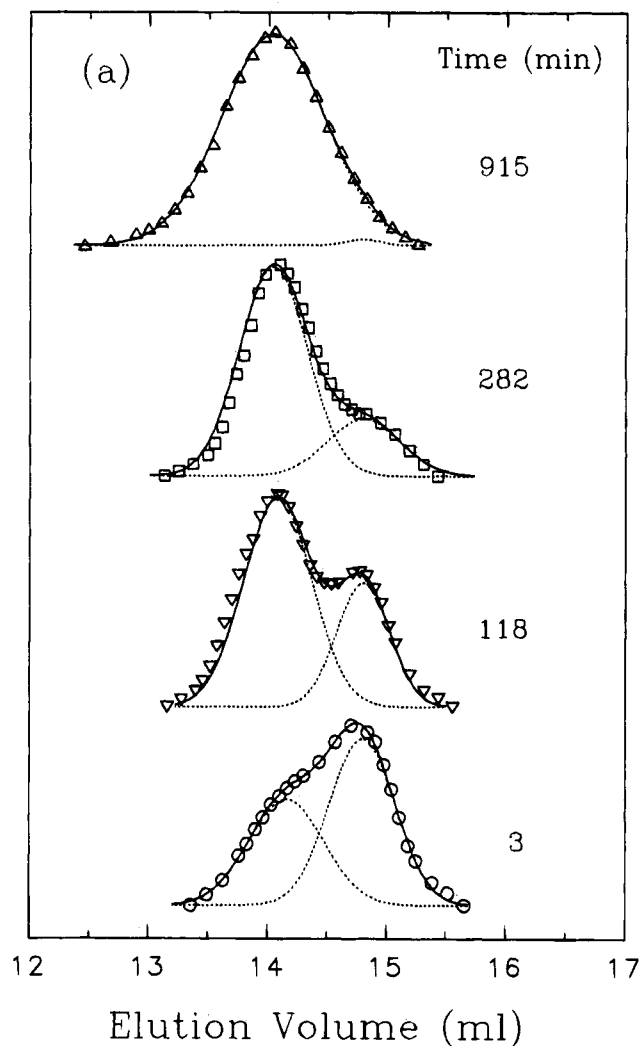


FIGURE 5: (a) Dependence of the elution profiles of H17Q in 1.5 M GdnHCl on the time of prior incubation in 1.5 M GdnHCl at 25 °C. A Superdex 75 column was used. The two peaks seen in the elution profiles at early times are at 14.8 and 14 mL. The elution volumes of H17Q in 0, 3, and 6 M GdnHCl are 14.8, 12.8, and 12 mL, respectively, on the Superdex 75 column. The elution profiles from panel a were deconvoluted into two Gaussian peaks (dotted lines). The solid lines through the elution profile data points are the sums of the two Gaussian peaks. Only four time points are shown. (b) Fractional areas of the two peaks in 1.5 M GdnHCl as a function of time of prior incubation. The relative area under each of the Gaussian peaks was determined and is plotted as a function of time of prior incubation in 1.5 M GdnHCl. This time does not include the time of chromatography which was 30 min. (∇) Relative area of the peak centered at 14.8 mL; (○) relative area of the peak centered at 14 mL. The solid lines are fits of the data to single exponentials, and both yield an apparent rate constant for interconversion between the two peaks of  $6.7 \times 10^{-5} \text{ s}^{-1}$ .

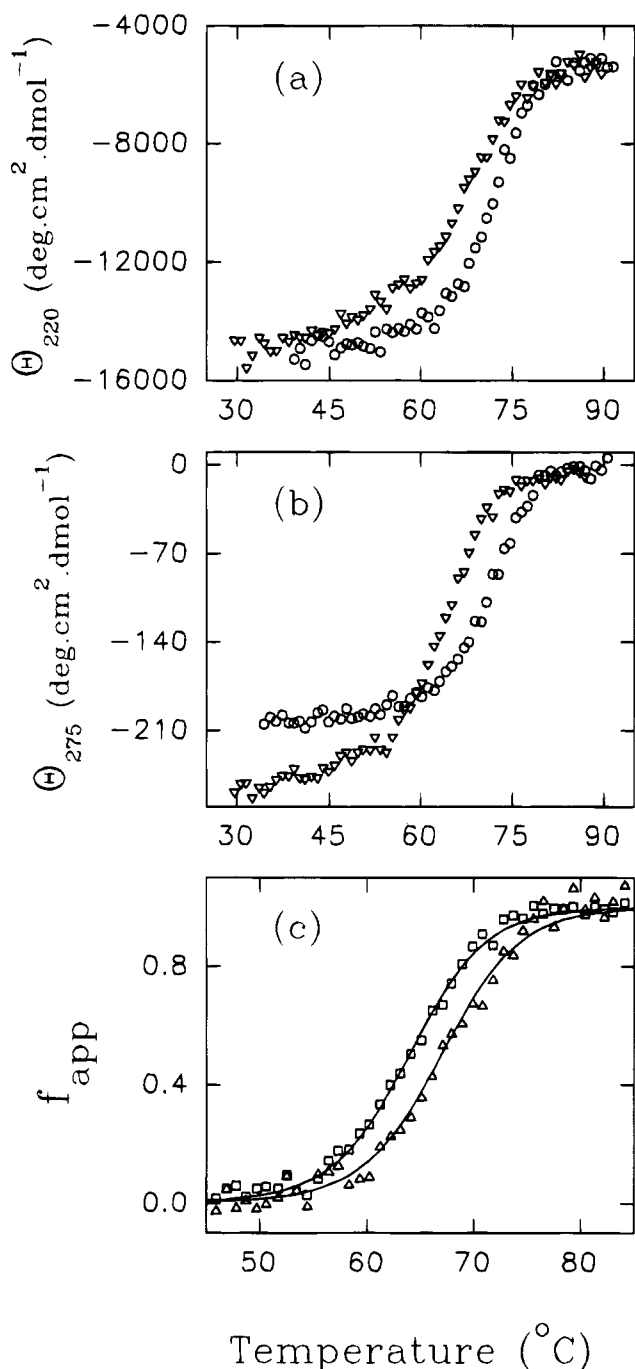


FIGURE 6: Thermal denaturation curves of H17Q and wt barstar at pH 7. (a) Thermal denaturation was followed by monitoring mean residue ellipticity at 220 nm. (○) wt barstar; (∇) H17Q. (b) Thermal denaturation was followed by monitoring mean residue ellipticity at 275 nm. (○) wt barstar; (∇) H17Q. (c) The data for H17Q in panels a and b were converted to  $f_{app}$  using eq 1 and plotted versus temperature. (□) near-UV CD; (∇) far-UV CD. The midpoints of the thermal transitions, obtained as the temperatures at which the first derivatives of the thermal denaturation curves display a maximum, are  $68.3 \pm 0.5$  °C (far-UV CD, H17Q),  $65.0 \pm 0.5$  °C (near-UV CD, H17Q, and  $71.5 \pm 0.5$  °C (far- and near-UV CD, wt barstar).

1976; Kuwajima, 1989) leads to the resulting apoproteins displaying equilibrium unfolding intermediates under mildly denaturing conditions, which are not displayed by the corresponding holoproteins. An alternative method for destabilizing the fully-folded protein with respect to a folding intermediate is through destabilizing mutations. Multiple site-directed mutations in barnase cause urea denaturation

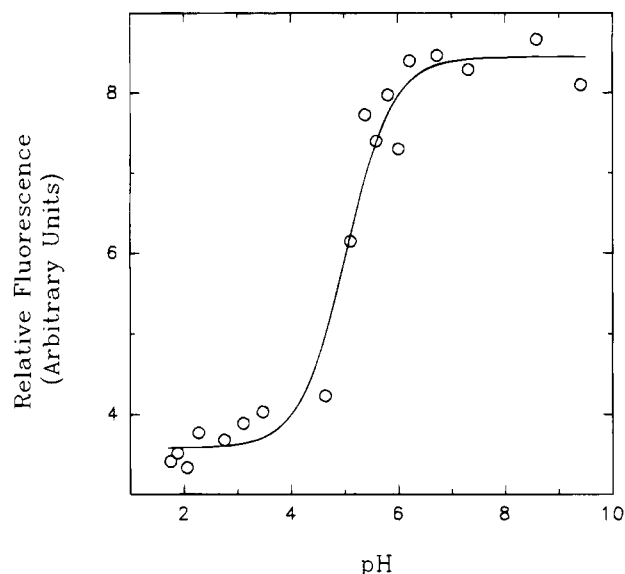


FIGURE 7: pH dependence of the fluorescence of H17Q. The protein concentration was  $2 \mu\text{M}$ . The solid line through the data is a nonlinear least-squares fit of the data to eq 9 and yielded a value for  $pH_m$ , the apparent  $pK_a$  of the transition, of  $5.0 \pm 0.2$ .

to proceed through an equilibrium unfolding intermediate (Sanz & Fersht, 1993), and site-directed mutagenesis has been used to further destabilize the fully-folded form relative to the equilibrium folding intermediate in the case of both apomyoglobin (Hughson & Baldwin, 1989) and the  $\alpha$ -subunit of tryptophan synthase (Chen *et al.*, 1992). In the case of the *trp* apopressor, a dimeric protein, mutation of a single *Trp* residue at the monomer–monomer interface populates a monomeric folding intermediate (Mann *et al.*, 1993), and in the case of  $\beta$ -lactamase, a single mutation causes the mutant protein to exist in a molten globule-like conformation in conditions where the wt protein is fully functional (Craig *et al.*, 1985). The data presented in Figures 3–6 show that the perturbation of a single specific tertiary hydrogen bond by mutagenesis of the sole His residue to a Gln in the single-domain protein barstar can cause at least one equilibrium folding intermediate I to be populated in the unfolding transition zone.

There are, of course, native proteins which undergo GdnHCl- or urea-induced denaturation through folding intermediates. Carbonic anhydrase B (Wong & Tanford, 1973),  $\alpha$ -lactalbumin (Kuwajima *et al.*, 1976),  $\beta$ -lactamase (Robson & Pain, 1976; Uversky & Ptitsyn, 1994),  $\beta$ -lactoglobulin (Anantanarayanan *et al.*, 1977), bovine growth hormone (Brems *et al.*, 1987), and DnaK (Palleros *et al.*, 1993) are examples of such proteins. In the case of apo  $\alpha$ -lactalbumin, carbonic anhydrase B, and bovine growth hormone, the intermediates observed in urea- or GdnHCl-induced unfolding appear to be similar to the molten globule form observed at low pH (Kuwajima, 1989). In the case of  $\beta$ -lactamase, a molten globule-like intermediate is observed upon unfolding by urea or GdnHCl only at 4 °C. Although barstar too forms a molten globule-like conformation at low pH, which binds ANS (Khurana & Udgaonkar, 1994), the intermediate I that forms on GdnHCl-induced or thermally induced denaturation of H17Q does not bind ANS (see Results). Although there is considerable secondary structure even with a disrupted tertiary structure in I, the disruption of the tertiary structure is not sufficient to permit the solvent exposure of hydrophobic surfaces to which ANS can bind.

It is also possible that there is sufficient disruption of the tertiary structure, but ANS does not bind because the negative charge of the protein at pH 7 repels ANS, which too has a negative charge.

His17 is in the first  $\alpha$ -helix of barstar that spans residue 12–25. The X-ray crystallographic structure of both the barnase–barstar complex (Guillet *et al.*, 1993) and uncomplexed barstar (Mauguen, Y., personal communication) shows that the N $\delta$ 1 atom of His17 is hydrogen bonded to the side chain hydroxyl group of Tyr30. The structure also shows that both His17 and Tyr30 are completely buried. Proton NMR studies of barstar in solution show that the His17 C $\beta$ -protons have strong nuclear Overhauser effect (NOE) connections to the Tyr30 ring protons, confirming the proximity of the side-chains to each other (S. Ramachandran and J. B. Udgaonkar, unpublished results). His17 is not involved in the interaction of barstar with barnase (Guillet *et al.*, 1993), and the His17→Gln17 mutation is therefore not expected to directly affect the interaction of barstar with barnase to any significant extent. The effect of the mutation on the change in absorption at 287 nm on unfolding (Figure 2c) and the mean residue ellipticity in the near-UV region (Figure 2b) can be attributed to the environment of Tyr30 being different in H17Q.

**GdnHCl-Induced Denaturation.** The data in Figure 3 show that tertiary structure is more unstable than secondary structure for the mutant protein H17Q. The  $C_m$  value obtained from the far-UV CD-monitored denaturation curve is the same as that reported earlier for wt barstar (Khurana & Udgaonkar, 1994; Shastry *et al.*, 1994), indicating that the mutation does not have any significant effect on the amount of secondary structure. This is supported by the observation that the mean residue ellipticity of the mutant protein at 222 nm, which is a measure of the amount of secondary structure, is virtually the same as that of the wt protein (Figure 2a). In contrast, the  $C_m$  value is lower by 0.4 M when obtained from the fluorescence-monitored denaturation curve and lower by 0.2 M when obtained from the near-UV CD-monitored denaturation curve.

The noncoincidence of the three denaturation curves, each monitored by a different optical probe, indicates that F unfolds to U through at least one equilibrium unfolding intermediate. It was not possible to fit the data in Figure 3 to a three-state model that includes only one intermediate form I (see Results). This suggests that I may not be unique, but may instead represent a collection of intermediates, and that gradual melting of the structure occurs with increasing GdnHCl concentration in the transition zone. Gradual melting of structure in the transition zone has in fact been observed in the case of the three-state unfolding of DnaK (Palleros *et al.*, 1993).

**Size Exclusion Chromatography.** The data in Figure 5a,b indicate that fully-folded H17Q converts to one or more slightly less compact forms (I) in 1.5 M GdnHCl in two kinetic phases. As long as both F and I are present, the slow exchange between them results in two separate elution peaks. Approximately 50% of F molecules convert to I within 3 min, the earliest time of chromatography. The remaining molecules of F slowly convert to I over a period of 900 min, and the area of the peak at which I elutes (14 mL) increases at the expense of the peak at which F elutes out (14.8 mL). The data indicate that after 15 h, all F has converted to I and U. The data in Figures 4a,b indicate that I is in fast

exchange with U. As the concentration of GdnHCl is increased, the concentration of U increases at the expense of I, and the single elution peak which is the weighted average of the elution volumes of I and U moves to where U elutes out. This suggests that in 1.5 M GdnHCl all of F transforms to I (Figure 5a,b) and that the predominant form present at equilibrium is I.

The gel filtration results do not, however, provide any definite indication as to whether I is a single intermediate or a collection of intermediates in rapid equilibrium with each other. Nonetheless, the observation that the conversion from F to I is biphasic suggests that I might represent more than one intermediate. If a single intermediate I is indeed present for H17Q in 1.5 M GdnHCl, and U and F are indeed populated to insignificant extents under these conditions, then Figure 3 indicates that in comparison to F, I has 75% of the far-UV mean residue ellipticity, 60% of the near-UV mean residue ellipticity, and 45% of the fluorescence. These optical properties of H17Q in 1.5 M GdnHCl were used to estimate  $Z_I$  using eq 5 (see Results) for a three-state analysis of the data in Figure 3 according to eq 4. Such a three-state analysis was, however, not successful (see Results), again indicating that I probably represents more than one intermediate.

The artifact seen at low concentrations of GdnHCl (Figure 4a,b) prevented a quantitative analysis of the denaturation reaction as monitored by gel filtration. This artifact does not, however, have any bearing on the data presented in Figure 5a, which clearly shows slow exchange between two forms of the protein. The more compact of these forms appears to be F, and the less compact form clearly cannot be U (Figure 4a) and must therefore represent I.

There are at least two kinetic intermediates, an early intermediate  $I_1$  and a later native-like intermediate,  $I_N$  on the major folding pathway of both barstar (Shastry *et al.*, 1994) and BSCCAA (Schreiber & Fersht, 1993), which are populated at concentrations of GdnHCl below the folding transition zone. At present, the relationship of I, which accumulates in the case of H17Q, to these kinetic intermediates is unknown. Kinetic experiments in progress should provide an answer.

**Thermally-Induced Denaturation.** At least one equilibrium intermediate is populated even during thermal denaturation. Again, tertiary structure as monitored by near-UV CD melts before secondary structure monitored by far-UV CD. Tertiary structure monitored by absorbance at 287 nm or by fluorescence at 332 nm on excitation at 287 nm melts even earlier (see Results). A simulated fitting of the thermal denaturation curves to the three-state model was attempted, as described by Kuroda *et al.* (1992), but was not successful because of the large number of unknown parameters. At present, it is also not possible to comment on the possibility of the intermediate(s) populated in the thermally-induced unfolding transition and the GdnHCl-induced unfolding transition being identical.

**Contribution of the His17-Tyr30 Hydrogen Bond to the Stability of Barstar.** There is some controversy about the contribution of hydrogen bonds on the surface of a protein to the stability of the protein (Alber *et al.*, 1988). Nevertheless, it has been clearly established both in the case of proteins (Alber *et al.*, 1987) and in the case of protein–ligand complexes (Fersht, 1987) that unpaired hydrogen bond donors or acceptors that are buried are destabilizing. Both

His17 and Tyr30 are buried; thus, the specific tertiary hydrogen bond between the side chains of these aromatic residues is expected to stabilize the protein. The specific hydrogen bond was perturbed by replacing His17 by Gln. Gln was chosen because it is similar in hydrophobicity to His and is commonly used as a replacement for His (Sali *et al.*, 1988). Moreover, its helix propensity is similar to that of His (Fasman, 1989; Richardson & Richardson, 1988), and the mutation was not expected to greatly perturb the stability of the helix. Thus, the His17-Gln17 mutation was expected to alter the stability of the tertiary structure to a greater extent than it would the stability of the secondary structure. A detailed analysis of the contribution of the His17-Tyr30 hydrogen bond to the stability of barstar has, however, not been attempted for several reasons.

In the first case, the single His17→Gln17 mutation may have perturbed other interactions yet to be identified beside the tertiary hydrogen bond (see, for example, Alber *et al.*, 1987; Grütter *et al.*, 1987). The amide group of Gln17 might in fact be replacing the His17 N $\delta$ 1 atom as the hydrogen bond acceptor in H17Q, but this hydrogen bond in H17Q would not be expected to make the same contribution to the stability as does the original specific hydrogen bond in wt barstar. More importantly, it has not been able to quantitatively determine the stability of fully-folded H17Q. The difficulty in doing so arises from the complexity of its unfolding. The data in Figure 3 do not satisfactorily fit a three-state model for unfolding with only one equilibrium intermediate between F and U and therefore suggest that I represents more than one equilibrium unfolding intermediate. The number of unknown parameters in a four-state model incorporating two intermediates is too large for the data to be reliably fit to such a model. In spite of the inability to carry out a quantitative analysis, as was desired, the results reported here clearly indicate the importance of the specificity of the His17-Tyr30 hydrogen bond in determining the stability of the tertiary structure of barstar.

**Role of His17 in the F→A Transition.** It has been previously shown the structural transition from the F state of barstar to the molten globule-like A form appears to be coupled to the protonation of a single titratable group (Khurana & Udgaonkar, 1994), and it was suspected that this group might be the sole His (His17) residue in the protein, which would then be expected to have an abnormally low pK<sub>a</sub> value in the F state. The aromatic side chain of His17 is buried, and its N $\delta$ 1 atom is involved in hydrogen bonding, and therefore a lowered pK<sub>a</sub> value is expected. NMR titrations of the chemical shifts of the ring protons of His17 in wt barstar do indeed indicate that the pK<sub>a</sub> value of His17 is shifted to below 5.8 (S. Ramachandran and J. B. Udgaonkar, unpublished results). It was not possible to carry out the NMR pH titration below the pH range 5.8–10 because of the very low solubility of barstar around pH 5, but chemical shifts of the ring protons of His17 do not even begin to titrate at pH 5.8. Since the A form of barstar too has partial secondary structure and a perturbed tertiary structure (Khurana & Udgaonkar, 1994) and also the His17→Gln17 mutation perturbs the tertiary structure more than it does the secondary structure, it was important to determine the effect of the mutation on the F→A transition.

It is seen in Figure 7 that the His17→Gln17 mutation has no effect on the structural transition between the F state and the A form: the transitions in both H17Q and wt barstar are

characterized by the same apparent pK<sub>a</sub> of 5.0 (see Figure 7). The amount of secondary structure in the A form of H17Q is also virtually the same as in the wt protein (data not shown). Thus, protonation of His17 in barstar does not appear to be involved in the F → A conformational change at low pH.

The ability to change any specific amino acid residue in the polypeptide sequence at will using site-directed mutagenesis has been widely exploited to study the roles of specific amino acid residue positions and specific interactions in determining the stability of folded proteins and folding intermediates (Matouschek & Fersht, 1991; Shortle, 1992; Matthews, B. W., 1993). The effect of the mutation on the stability of the protein has usually been determined with the assumption that the mutant protein unfolds by the same two-state U ⇌ F transition as does the wild-type protein: only one structural probe is usually used to monitor the denaturation process from which the stability of the protein is determined. The importance of confirming the two-state model for the unfolding of mutant proteins has been stressed by Hawkes *et al.* (1984). It is shown here that a single mutation in the small monomeric, single-domain protein, barstar, can indeed destabilize the fully-folded protein sufficiently with respect to a folding intermediate I so that the intermediate accumulates to an appreciable extent in equilibrium conditions.

In summary, it has been shown that perturbation of a specific tertiary hydrogen bond in barstar, by replacement of one of the hydrogen-bonding partners His17 by Gln, leads to accumulation of an equilibrium folding intermediate. Conditions have been established in which the folding intermediate is the predominant form of the protein present. Present studies are targeted toward using proton NMR to study the structure of this partly-folded equilibrium intermediate in which tertiary structure is perturbed to a greater extent than secondary structure.

#### ACKNOWLEDGMENT

We thank Doug Barrick for introducing us to the PCR-based site-directed mutagenesis method and for help in getting us started; B. R. Krishan for assistance in purifying the mutant protein; Mathew K. Mathew and Raghavan Varadarajan for useful discussions; C. Ramkrishnan for determining for us the degree of buriedness of the residues in barstar; and Robert Baldwin, Mathew K. Mathew, and Raghavan Varadarajan for their comments on various versions of the manuscript. J.B.U. is the recipient of a Biotechnology Career Fellowship from the Rockefeller Foundation.

#### REFERENCES

- Alber, T., Sun, D.-P., Wilson, K., Wozniak, J. A., Cook, S. P., & Matthews, B. W. (1987) *Nature* 330, 41–46.
- Alber, T., Bell, J. A., Sun, D.-P., Nicholson, H., Wozniak, J. A., Cook, S. P., & Matthews, B. W. (1988) *Science* 239, 631–635.
- Anantanarayanan, V. S., Ahmad, F., & Bigelow, C. C. (1977) *Biochem. Biophys. Acta* 492, 194–203.
- Barrick, D., & Baldwin, R. L. (1993) *Biochemistry* 32, 3790–3796.
- Bradford, M. M. (1976) *Anal. Biochem.* 72, 248–254.
- Brems, D. N., Plaisted, S. M., Dougherty, J. J., & Holzman, T. F. (1987) *J. Biol. Chem.* 262, 2590–2596.

- Chen, X., Rambo, R., & Matthews, C. R. (1992) *Biochemistry* 31, 2219–2223.
- Craig, S., Hollecker, M., Creighton, T. E., & Pain, R. H. (1985) *J. Mol. Biol.* 185, 681–687.
- Dobson, C. M. (1994) *Curr. Biol.* 4, 636–640.
- Evans, P. A., & Radford, S. E. (1994). *Curr. Opin. Struct. Biol.* 4, 100–106.
- Fasman, G. D. (1989) in *Prediction of Protein Structure and the Principles of Protein Conformation* (Fasman, G. D., Ed.) pp 193–307, Plenum, New York.
- Fersht, A. R. (1987) *Trends Biochem. Sci.* 12, 301–304.
- Garvey, E. P., & Matthews, C. R. (1989) *Biochemistry* 28, 2083–2093.
- Grütter, M. G., Gray, T. M., Weaver, L. H., Alber, T., Wilson, K., & Matthews, B. W. (1987) *J. Mol. Biol.* 197, 315–329.
- Guillet, V., Laphorn, A., Hartley, R. W., Mauguen, Y. (1993) *Structure* 1, 165–176.
- Hartley, R. W. (1988) *J. Mol. Biol.* 202, 913–915.
- Hawkes, R., Grutter, M. G., & Schellman, J. (1984) *J. Mol. Biol.* 175, 195–212.
- Hughson, F. M., & Baldwin, R. J. (1989) *Biochemistry* 28, 4415–4422.
- Khurana, R., & Udgaonkar, J. B. (1994) *Biochemistry* 33, 106–115.
- Kim, P. S., & Baldwin, R. L. (1990) *Annu. Rev. Biochem.* 59, 631–660.
- Kirby, E. P., & Steiner, R. F. (1970) *J. Biol. Chem.* 245, 6300–6306.
- Kuroda, Y., Kidokoro, S., & Wada, A. (1992) *J. Mol. Biol.* 223, 1139–1153.
- Kuwajima, K. (1989) *Proteins: Struct., Funct., Genet.* 6, 87–103.
- Kuwajima, K. (1992) Protein folding *in vitro*. *Curr. Opin. Biotechnol.* 3, 462–467.
- Kuwajima, K., Nitta, K., Yoneyama, M., & Sugai, S. (1976) *J. Mol. Biol.* 106, 359–373.
- Lubienski, M. J., Bycroft, M., Freund, S. M. V., & Fersht, A. R. (1994) *Biochemistry* 33, 8866–8877.
- Mann, C. J., Royer, C. A., & Matthews, C. R. (1993) *Protein Sci.* 2, 1853–1861.
- Matouschek, A., & Fersht, A. R. (1991). *Methods Enzymol.* 202, 82–112.
- Matthews, B. W. (1993) *Annu. Rev. Biochem.* 62, 139–160.
- Matthews, C. R. (1993) *Annu. Rev. Biochem.* 62, 653–683.
- Merino, E., Osuna, J., Bolivar, F., & Soberon, X. (1992) *BioTechniques* 12, 508–509.
- Mossakowska, D. E., Nyberg, K., & Fersht, A. R. (1989) *Biochemistry* 28, 3843–3850.
- Osterman, H. L., & Walz, F. G., Jr. (1978) *Biochemistry* 17, 4124–4130.
- Pace, C. N., Shirley, B. A., & Thomson, J. A. (1989) in *Protein Structure: A Practical Approach* (Creighton, T. E., Ed.) pp 311–330, IRL Press, Oxford, UK.
- Paddon, C. J., & Hartley, R. W. (1987) *Gene* 53, 11–19.
- Palleros, D. R., Shi, L., Reid, K. L., & Fink, A. L. (1993) *Biochemistry* 32, 4314–4321.
- Privalov, P. L. (1992) in *Protein Folding* (Creighton, T. E., Ed.) pp 83–126, W. H. Freeman & Co., New York.
- Ptitsyn, O. B. (1992) in *Protein Folding* (Creighton, T. E., Ed.) pp 243–300, W. H. Freeman & Co., New York.
- Richardson, J. S., & Richardson, D. C. (1988) *Science* 240, 648–6.
- Robson, B., & Pain, R. H. (1976) *Biochem. J.* 155, 322–330.
- Roder, H., Elöve, G. A., & Englander, S. W. (1988). *Nature* 335, 700–704.
- Šali, D., Bycroft, M., & Fersht, A. R. (1988) *Nature* 335, 740–743.
- Sambrook, J., Fritsch, E. F., & Maniatis, T. (1989) in *Molecular Cloning: A Laboratory Manual*, 2nd ed. Vol. 1, pp 1.74–1.84, Cold Spring Harbor Laboratory Press, Cold Spring Harbor, NY.
- Sanger, F., Nicklen, S., & Coulson, A. R. (1977) *Proc. Natl. Acad. Sci. U.S.A.* 74, 5463–5467.
- Santoro, M. M., & Bolen, D. W. (1988) *Biochemistry* 27, 8063–8068.
- Sanz, J. M., & Fersht, A. R. (1993) *Biochemistry* 32, 13584–13592.
- Schagger, H., & von Jagow, G. (1987) *Anal. Biochem.* 166, 368–379.
- Schellman, J. A. (1978) *Biopolymers* 17, 1305–1322.
- Schreiber, G., & Fersht, A. R. (1993) *Biochemistry* 32, 11195–11203.
- Shastry, M. C. R., Agashe, V. R., & Udgaonkar, J. B. (1994) *Protein Sci.* 3, 1409–1417.
- Shortle, D. (1992) *Q. Rev. Biophys.* 25, 205–250.
- Shortle, D., Meeker, A. K., & Freire, E. (1988) *Biochemistry* 27, 4761–4768.
- Stryer, L. (1965) *J. Mol. Biol.* 13, 482–495.
- Udgaonkar, J. B., & Baldwin, R. L. (1988) *Nature* 335, 694–699.
- Uversky, V. N., & Ptitsyn, O. B. (1994) *Biochemistry* 33, 2782–2791.
- Wong, K.-P., & Tanford, C. (1973) *J. Biol. Chem.* 248, 8518–8523.
- Zitzewitz, J. A., & Matthews, C. R. (1993) *Curr. Opin. Struct. Biol.* 3, 594–600.

BI941821H